

## Damage-based optimal design of friction dampers in multistory chevron braced steel frames



Farshad Taiyari<sup>a,1</sup>, Federico M. Mazzolani<sup>b</sup>, Saman Bagheri<sup>a,\*</sup>

<sup>a</sup> Faculty of Civil Engineering, University of Tabriz, 51666-16471 Tabriz, Iran

<sup>b</sup> Department of Structures for Engineering and Architecture, University of Naples "Federico II", P.le Tecchio 80, 80125 Naples, Italy

### ARTICLE INFO

#### Keywords:

Friction damper  
Nonlinear dynamic analysis  
Seismic fragility  
Slip force  
Damage probability

### ABSTRACT

In this paper, a probability-based design methodology of the friction dampers in multi-story steel frames is proposed. Both the slip force of the device and the stiffness ratio of the system are analyzed as two important parameters, which affect the behavior of the structures equipped with friction devices. The seismic fragility of friction damped braced frames is evaluated and used to identify the optimal ranges of the above-mentioned design parameters so as to minimize the overall damage probability of the structure under the action of strong ground motions. For this purpose, fragility functions of the structural models are derived using nonlinear incremental dynamic analyses. To demonstrate the efficiency of the proposed method, three structural models of steel moment resisting frames with friction damper systems (including chevron braces and damper devices) are considered for the purpose of the seismic performance analysis. The results of the analyses show that the largest damage probability in each structural model corresponds to the case with the higher slip force and the lower stiffness ratio, where the undesirable buckling failure will govern before full activation of friction damper. For the three considered building frames, the optimal range of slip force lies between 40% and 55% of the total weight of structures and the recommended value for stiffness ratio is 2.

### 1. Introduction

Since several decades the seismic response control techniques have been used as complementary solutions to the existing seismic force resisting systems and several types of passive energy dissipation devices have been developed. Friction dampers are considered one of the most effective passive control devices for building structures against earthquake actions. Compared to the velocity-dependent devices, such as viscous and viscoelastic dampers, friction dampers provide energy-dissipation capacity with a sufficient lateral stiffness. The action of these dampers is based on the mechanism of dry friction which develops between two solid bodies, sliding relatively one to another for providing a specified energy dissipation capacity [1]. The friction devices exhibit hysteretic behaviors similar to those achieved by the metallic devices.

Recently, considerable progress has been made in the development of this type of devices. Pall friction damper is the most commonly and widely used type of friction dampers, which was originally introduced by Pall et al. [2,3], based upon the automotive brake. It can be located in structures either as a part of braces [4] or, more recently, as beam-to-

column joints [5,6]. The friction devices basically consist of steel plates tightened together by means of high strength steel bolts, whose either axial or rotational deformation mechanisms lead to a transformation of kinetic energy into thermal energy; so, the maximum amount of friction force can be controlled by adjusting the friction coefficient of the sliding surfaces, as well as the compression force of the tightened bolts, but it is independent of the sliding velocity and the contact area of the sliding surface.

Since the 90s of the last Century, Sumitomo Metal Industry in Japan developed a different type of friction dampers [7]. This device consists of copper pads impregnated with graphite in contact with the wedges inside of the steel cylinder. The load on the contact surface is induced by a series of wedges that act under the compressive force of the Belleville washer springs (cup springs). The graphite serves as a lubricant between the contact surfaces and ensures a stable coefficient of friction and silent operation. The experimental study of Aiken and Kelly [7] allows the Sumitomo damper to be used as a structural damper system. They compared the response of moment resisting frames without and with this damper. Their findings showed that the energy dissipation is mainly due to the action of friction in the damper device rather than

\* Corresponding author.

E-mail addresses: [farshad.taiyari@unina.it](mailto:farshad.taiyari@unina.it) (F. Taiyari), [fmf@unina.it](mailto:fmf@unina.it) (F.M. Mazzolani), [s\\_bagheri@tabrizu.ac.ir](mailto:s_bagheri@tabrizu.ac.ir) (S. Bagheri).

<sup>1</sup> Visiting scholar, Department of Structures for Engineering and Architecture, University of Naples "Federico II", P.le Tecchio 80, 80125 Naples, Italy.

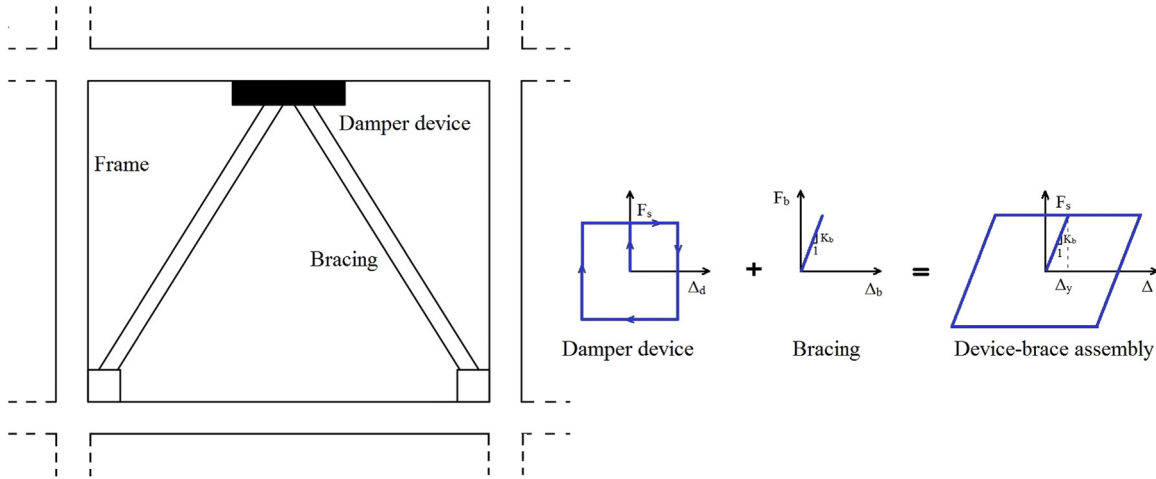


Fig. 1. Typical location and behavior of a friction damper device in a story frame.

due to the inelastic action of the structural members. The low-cost slotted bolted dampers [8] are also introduced as a type of friction damper mostly installed at one end of bracing members. It comprises a series of steel plates (e.g. a gusset plate, two back-to-back channels, and cover plates) bolted together with a specified tightening force. Another common type of friction dampers is EDR (Energy Dissipating Restraint) [9], which uses steel and bronze friction wedges to convert the axial spring force into normal pressure on the cylinder. Different hysteresis behaviors can be reached by tuning the spring constant, the core configuration, the initial slip force, and the gap size. Zhou and Peng [10] proposed a new friction-variable damper based on the EDR device, where both springs and wedges are replaced by a sliding shaft and a friction ring, while two zones with high and low friction coefficient are inserted into the internal walls of the external cylinder. Mualla and Nielsen [11] introduced another type of friction dampers called Friction Damper Device (FDD), which consists of a central (vertical) plate, two side (horizontal) plates, with two circular friction pads between the steel plates. Golafshani et al. [12] investigated the potential application of the FDD damper in offshore jacket structures. More recently, a novel combined system of amplified added stiffness and damping (AASD), consisting of an amplifying mechanism and a frictional self-centering damper capable to support large displacements, has been analyzed and tested in full scale [13].

Despite their wide-spread applications, design guidelines for structures equipped with supplemental energy dissipation devices are still in a developing phase. An important design parameter of the friction damper devices is their slip force, which highly affects the structural response. Recently, several studies have been conducted in order to optimize the slip force of the device and, therefore, its energy dissipation capacity. Filiatrault and Cherry [14] proposed an optimal solution for minimizing the strain energy in structural members. They also presented several design spectra as a function of structural and ground motion properties to estimate the slip force of friction damper devices [15]. Fu and Cherry [16] also modified the codified lateral load distribution for an optimal design of structures equipped with friction damper systems; this method allows to obtain proper values of damper slip forces, yield displacement of frame (in order to satisfy its ductility demand) and stiffness of the whole structure, including devices and their supporting braces. The more advanced numerical methods focus the attention to improve the optimization of damper parameters more than before [17–19]. In all of these studies, one or more engineering demand parameters (EDPs) of structures (e.g. inter-story drift, floor acceleration or velocity) are used as a cost function.

In this paper, a new approach, which considers the overall damage probability (potential) of structures as a cost function, is presented for the optimum design of friction dampers in steel moment resisting

frames. The damage probability of a structure is evaluated by the aid of fragility function. The slip force of the damper device and the stiffness ratio of the system are chosen as design variables while a wide variety of these parameters in the applicable ranges are examined to better understand the structural behavior and to find the best performance. As illustrative numerical examples, friction damped braced frames with different number of stories (3, 6, and 9) are modeled in OpenSees software and incremental dynamic analyses (IDA) are performed on these models. Finally, the 50% probability of collapse is evaluated for all the analyzed models, leading to a selection of an optimal range of damping system parameters.

## 2. Friction damped braced frames

It is well known that the relative sliding between two surfaces in contact produces energy dissipation through friction, which depends on a wide variety of parameters such as surface finishing, relative velocity, temperature, confinement pressure, and loading history. Depending on the installed support, friction dampers can be incorporated in X-type or diagonal braces, or mounted on chevron braces [1].

Fig. 1 represents one bay of a structural frame equipped with a friction damper. Herein, the damper device is installed to the frame by the aid of chevron bracing as a supporting system and the combination is called the device-brace assembly. It is clear that the device and the supporting braces are connected in series and the device-brace assembly works in parallel with the structural frame (see Fig. 1). Therefore, with considering the Coulomb's law for modeling friction damper, its stiffness before slip ( $k_d$ ) is approximately equal to infinity; so, the total stiffness of device-brace assembly ( $k_{bd}$ ) is equal to the brace stiffness ( $k_b$ ), as given in Eq. (1). When frame plus braces are designed to perform in the elastic ranges, Eq. (2) can be used for estimating the slip force of the damper device. Based on the mentioned formula, the design parameters of interest for such an assembly are: the slip force of the damper device  $F_s$ , the displacement of the brace at which the device starts to slip  $\Delta_y$ , and the stiffness ratio  $SR$ , which is defined in Eq. (3) as a ratio of the device-brace assembly stiffness (which is equal to the brace stiffness), to bare frame stiffness  $k_s$  [18]. However, for a given frame with a fixed stiffness, only two of these parameters are independent since the third one can be determined from Eq. (2).

$$k_{bd} = \frac{1}{\left(\frac{1}{k_b}\right) + \left(\frac{1}{k_d}\right)} \xrightarrow{k_d=\infty} k_{bd} = k_b \quad (1)$$

$$F_s = k_{bd}\Delta_y = k_b\Delta_y = SRk_s\Delta_y \quad (2)$$

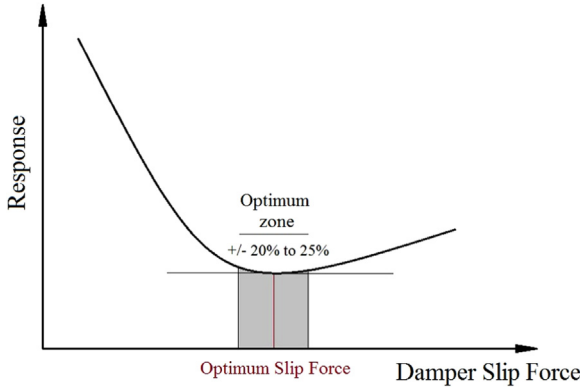


Fig. 2. Response versus slip load [20].

$$SR = \frac{k_{bd}}{k_s} = \frac{k_b}{k_s} \quad (3)$$

The response of structures with friction dampers are highly influenced by their slip forces. Selected slip force must be high enough to avoid damper slippage in small values of the applied lateral loads, while it must be low enough to enable slippage before yielding of main structural elements. For an optimal design, a series of analyses should be performed to determine an optimum slip force of the friction dampers to achieve a minimum response. Previous studies have shown that variations up to  $\pm 20\%$  of the optimum slip force do not significantly affect the response (see Fig. 2) [20].

### 3. Fragility function

A fragility function gives the probability of collapse, or other limit states of interest, of a structure as a function of some ground motion intensity measure (*IM*). The parameter *IM* is often quantified by the spectral acceleration with a specified period and damping or by peak ground acceleration (PGA). An estimated fragility function can also be combined with a ground motion hazard curve to evaluate the mean annual rate of collapse in a structural system [21].

There are several methods to perform nonlinear dynamic structural analyses to collect the data for estimating a fragility function. Recently, the most common approach is using incremental dynamic analysis (IDA), where a series of ground motions is repeatedly scaled in order to find the *IM* level at which each ground motion causes collapse or exceedance of a specific limit state [22]. For a given ground motion and dynamic analysis result, the collapse potential of a structure is usually correlated with the structural response parameters, such as roof or story drift, or directly defined based on the ground motion intensity at which the structure will become dynamically unstable [23]. A mathematical approach to present fragility function based on the above-mentioned definitions is given as:

$$Fragility = P[LS|IM = x] \quad (4)$$

where, *LS* represents the collapse or a specified limit state of the structural system, *IM* is the ground motion intensity measure, and *x* represents a specific value of *IM*.

Damage probability at a given *IM* level can be directly computed as:

$$P[EDP \geq LS|IM] = \frac{n}{N} \quad (5)$$

where, *N* is the total number of applied ground motion records and *n* is the number of cases that the defined limit state(s) is (are) exceeded. In most cases, fragility data can be fitted well with a lognormal cumulative distribution function:

$$P[EDP \geq LS|IM] = \Phi\left(\frac{\ln(x/\theta)}{\beta}\right) \quad (6)$$

where,  $\Phi()$  is the standard normal cumulative distribution function,  $\theta$  is the median of the fragility function (the *IM* level with 50% probability of damage), and  $\beta$  is the standard deviation of  $\ln(IM)$ .

### 4. A method of estimating design parameters of friction damper-brace assembly

The main purpose of this study is to find the optimum parameters of friction damping systems in multi-story frames by using fragility functions. As mentioned earlier, the behavior of device-brace assembly is mostly influenced by two independent variables: the slip force of the damper device,  $F_s$ , and the stiffness ratio, *SR*. The distribution of slip forces and stiffness ratios along the height of the multi-story building structure is assumed to be uniform in this study. Thus, the total slip force of all damper devices of a building with *ns* number of stories is  $ns \times F_s$ . This parameter can be normalized by dividing it by the total weight of the structure:

$$\bar{F}_s = \frac{nsF_s}{W_t} \quad (7)$$

where  $\bar{F}_s$  is the normalized slip force of damper devices and  $W_t$  is the total weight of the building. If the weight of each story is the same (i.e.  $W = W_t/ns$ ), the above equation and the definition of the normalized slip force can be simplified to:

$$\bar{F}_s = \frac{F_s}{W} \quad (8)$$

Therefore, two discrete design variables, i.e.  $\bar{F}_s$  and *SR*, is considered for each given multi-story building model to evaluate and to minimize its overall damage potential under the action of strong ground motions. After estimating these two non-dimensional design parameters, characteristics of the damper devices and their supporting braces in all stories of a given building frame can be obtained. In order to minimize the overall damage probability, the *IM* level with 50% probability of damage (i.e., the median of the fragility function) is considered here as an objective function, which should be maximized in the discrete design space of the variables  $\bar{F}_s$  and *SR*.

### 5. Illustrative examples and parametric study

#### 5.1. Design and modeling of structures

As study cases, 3, 6 and 9 story steel moment resisting frames (SMRF) with three bays of 5 m and story height of 3.2 m are designed according to AISC [24]. The gravity and live loads of all floors are assumed to be 4.5 and 2 kN/m<sup>2</sup>, respectively. The earthquake design force is calculated according to ASCE07 [25], considering the following parameters: importance factor  $I_e = 1$  (for residential buildings: Risk Category II), Site Class D (stiff soil), Seismic Design Category D, and response modification factor  $R = 4.5$  (for intermediate SMRF). The buildings are assumed to be located in Berkeley, CA. Then, a supplemental friction damper system (device-brace assembly) is added to each building frame (SMRFD). Fig. 3 shows the typical configuration of SMRFD models used in the current study. As it can be seen, damper devices are located in the mid-bay of the perimeter frames.

A two-dimensional model of each frame structure is created in OpenSees software to perform nonlinear dynamic analyses. Beam-to-column connections are assumed to be rigid. Both material and geometric nonlinearities are considered. The steel member material is A36, with elasticity modulus of 200 GPa and yield and ultimate strengths of 250 and 400 MPa, respectively. The stress-strain relationship of this material is defined by the *uniaxialMaterial Steel02* option in OpenSees. Beam, column and brace elements are modeled with *element forceBeamColumn* option in OpenSees. The P-delta effect is included in the analyses as a source of geometric nonlinearity. The multi-element brace members with fiber sections are used according to Fig. 4 to take

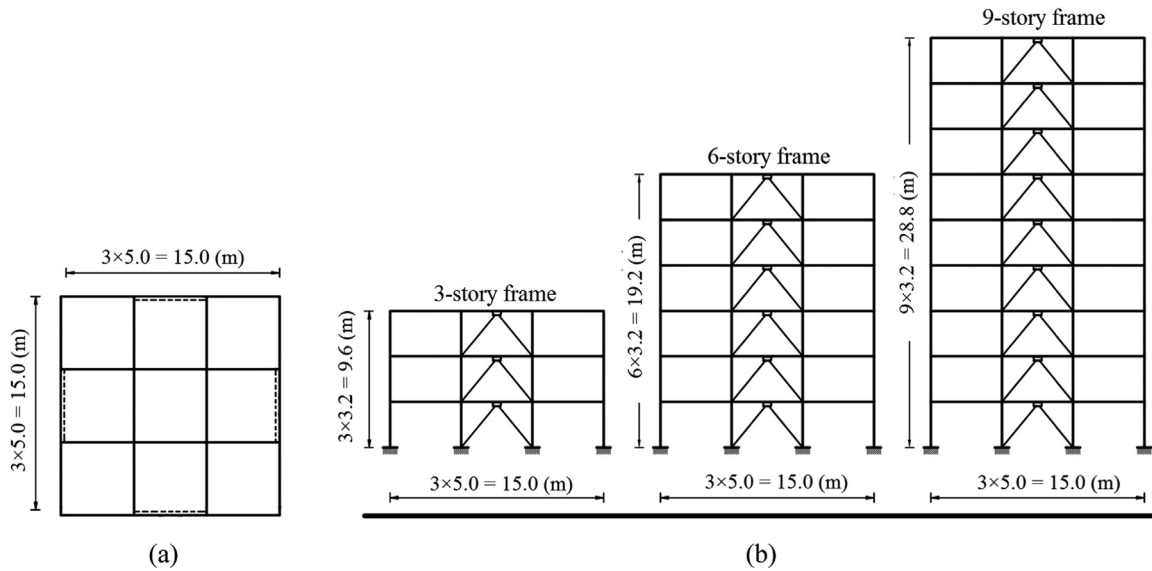


Fig. 3. Configuration of SMRFDs: (a) plan and (b) elevation views.

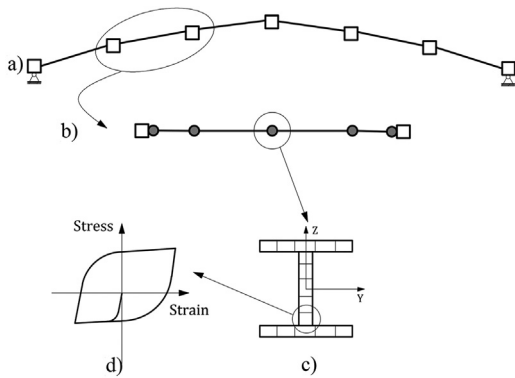


Fig. 4. Schematic illustration of a multi-element brace model: (a) initial camber of  $L/500$ ; (b) integration points; (c) cross-section subdivision; (d) uniaxial material model.

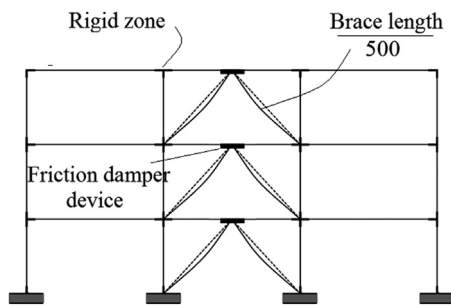


Fig. 5. Details of modeling a SMRFD in the OpenSees software.

into account for buckling of bracings. An initial camber is necessary for this purpose. Fig. 5 shows the details of modeling a SRMFD in the OpenSees software.

The hysteretic behavior of a friction damper device is illustrated in Fig. 6. This ideal rigid-plastic behavior is according to the coulomb's law. Such a behavior with a very small post yield stiffness ratio ( $= 0.0001$ ) and a very large elastic stiffness ( $= 1000 \text{ m}^{-1} \times$  damper slip force) is also recommended by Pall company [26] for computer modeling of Pall friction dampers supported by chevron braces.

In order to investigate the effects of design variables of friction damper systems (device-brace assemblies) on the seismic response and

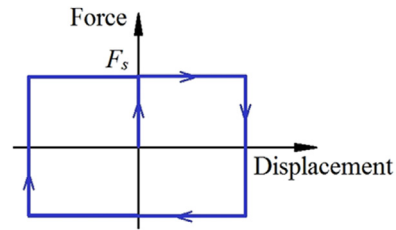


Fig. 6. Typical hysteretic behavior of friction damper.

damage probability of building structures as well as to identify the optimum damper design, parametric studies are conducted on the three frame models. For this purpose, the normalized slip forces are selected to vary between 0.1 (10%) and 1 (100%) with an interval of 0.1 (10%) and the stiffness ratios are changed from 1 to 5 with an interval of 1. Higher values of  $SR$  are not economically attractive. One additional value of  $\bar{F}_s$  is also analyzed in the middle of the critical interval of  $\bar{F}_s$ , if necessary. A SMRFD model with the specified values of  $ns$ ,  $\bar{F}_s$ , and  $SR$  is hereafter referred to as SMRFD- $ns/\bar{F}_s/SR$ . For example, SMRFD-3/20/2 represents a 3-story building frame model equipped with the friction damper system with a normalized slip force of 20% and a stiffness ratio of 2.

### 5.2. Ground motion records and limit states

A set of 22 far-field ground motion records of FEMA-P695 [27] are adopted here for IDA procedure. They come from sites located at greater than or equal to 10 km from fault rupture. Each record includes two horizontal components, but only the component with the larger value of peak ground acceleration (PGA) is used in this study. Table 1 summarizes the key information of these records.

The input earthquakes are characterized by the intensity measure ( $IM$ ), which is usually selected as the PGA or  $S_a(T_1, \xi = 5\%)$ . Both PGA and  $S_a(T_1, \xi = 5\%)$  are used in this study to interpret the IDA results. For the IDA procedure, the selected ground motion records are scaled to several  $IM$  levels, from  $PGA = 0.1 g$  with an increment of  $0.1 g$ , until the predefined damage state occurs. Two different limit states of damage are considered: (i) maximum inter-story drift ratio of 2% (corresponding to the life safety performance level) and (ii) global dynamic instability of the structure.

**Table 1**  
List of selected ground motions.

ID no.	Earthquake	Station	Year	M	PGA (g)	Site class (NEHRP)	Fault type
1	Northridge	Beverly Hills - Mulhol	1994	6.7	0.52	D	Thrust
2	Northridge	Canyon Country-WLC	1994	6.7	0.48	D	Thrust
3	Duzce, Turkey	Bolu	1999	7.1	0.82	D	Strike-slip
4	Hector Mine	Hector	1999	7.1	0.34	C	Strike-slip
5	Imperial Valley	Delta	1979	6.5	0.35	D	Strike-slip
6	Imperial Valley	El Centro Array #11	1979	6.5	0.38	D	Strike-slip
7	Kobe, Japan	Nishi-Akashi	1995	6.9	0.51	C	Strike-slip
8	Kobe, Japan	Shin-Osaka	1995	6.9	0.24	D	Strike-slip
9	Kocaeli, Turkey	Duzce	1999	7.5	0.36	D	Strike-slip
10	Kocaeli, Turkey	Arcelik	1999	7.5	0.22	C	Strike-slip
11	Landers	Yermo Fire Station	1992	7.3	0.24	D	Strike-slip
12	Landers	Coolwater	1992	7.3	0.42	D	Strike-slip
13	Loma Prieta	Capitola	1989	6.9	0.53	D	Strike-slip
14	Loma Prieta	Gilroy Array #3	1989	6.9	0.56	D	Strike-slip
15	Manjil, Iran	Abbar	1990	7.4	0.51	C	Strike-slip
16	Superstition Hills	El Centro Imp. Co.	1987	6.5	0.36	D	Strike-slip
17	Superstition Hills	Poe Road (temp)	1987	6.5	0.45	D	Strike-slip
18	Cape Mendocino	Rio Dell Overpass	1992	7.0	0.55	D	Thrust
19	Chi-Chi, Taiwan	CHY101	1999	7.6	0.44	D	Thrust
20	Chi-Chi, Taiwan	TCU045	1999	7.6	0.51	C	Thrust
21	San Fernando	LA - Hollywood Stor	1971	6.6	0.21	D	Thrust
22	Friuli, Italy	Tolmezzo	1976	6.5	0.35	C	Thrust

**6. Results and discussion**

Incremental dynamic analyses are performed for the 165 cases, by varying the normalized slip force (11 values) and the stiffness ratio (5 values) in the three structural models. Each IDA curve ends when it reaches the maximum inter-story drift of 2% or with a characteristic “flatline” which indicates that the maximum inter-story drift rapidly increases toward infinite values for small changes in *IM*, thus signaling global dynamic instability in the structural model. Figs. 7 and 8 depict the IDA curves for 6-story frame model with the normalized slip forces of 40% and 80% and the stiffness ratios of 2 and 4. As mentioned

earlier, both PGA and  $S_a(T_1, 5\%)$  have been used as the *IM* in the analysis results. As it can be seen, using  $S_a(T_1, 5\%)$  as an intensity measure, reduces the dispersion in the initial elastic region but not in the other parts, when the nonlinearity comes into play. Figs. 7 and 8 also indicate that when a higher value (i.e. 80%) is assumed for  $\bar{F}_s$ , the patterns of the IDA curves and their terminations levels of *IM* change considerably by increasing *SR* from 2 to 4. However, when a lower value of 40% is selected for  $\bar{F}_s$ , the overall results seem not to be very sensitive to the choice of *SR*. This will be further discussed later in this section.

The fragility data obtained using the IDA procedure as well as the

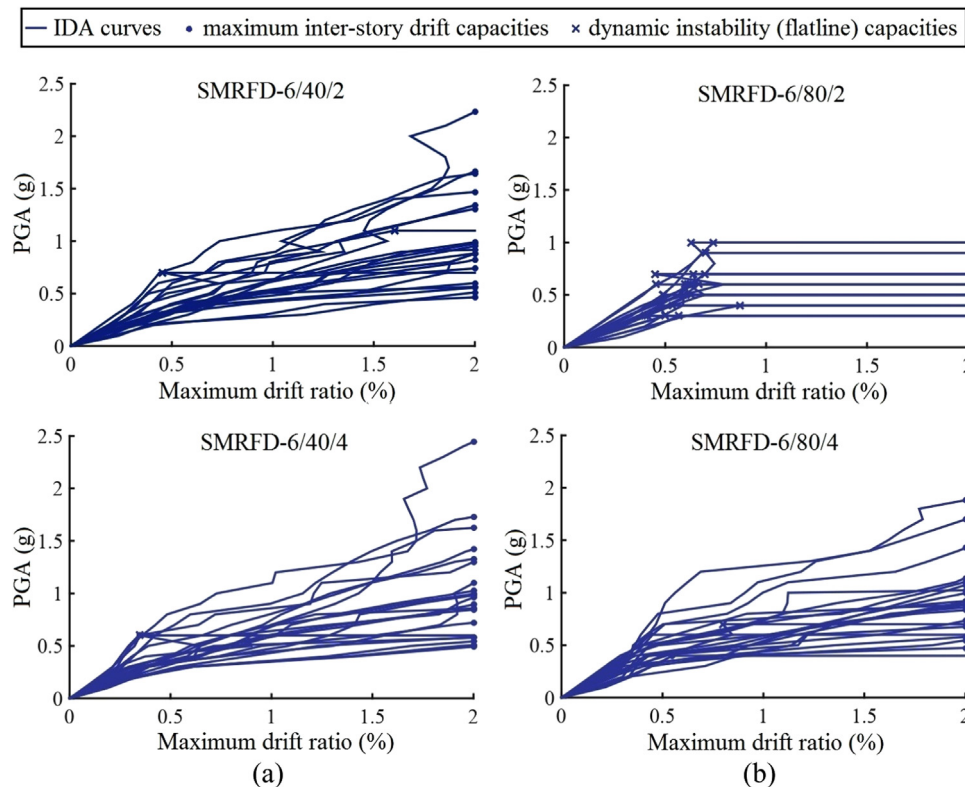


Fig. 7. IDA curves with *IM* = PGA: (a) SMRFD-6/40/2,4 and (b) SMRFD-6/80/2,4 models.

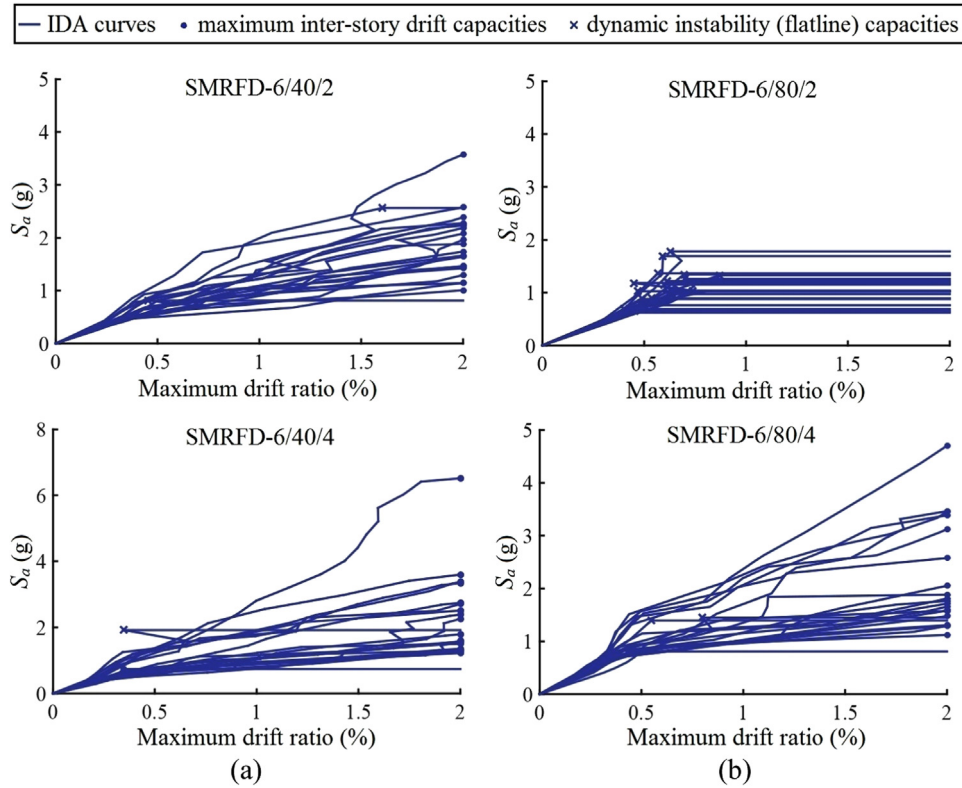


Fig. 8. IDA curves with  $IM = S_a(T_1, 5\%)$ : (a) SMRFD-6/40/2,4 and (b) SMRFD-6/80/2,4 models.

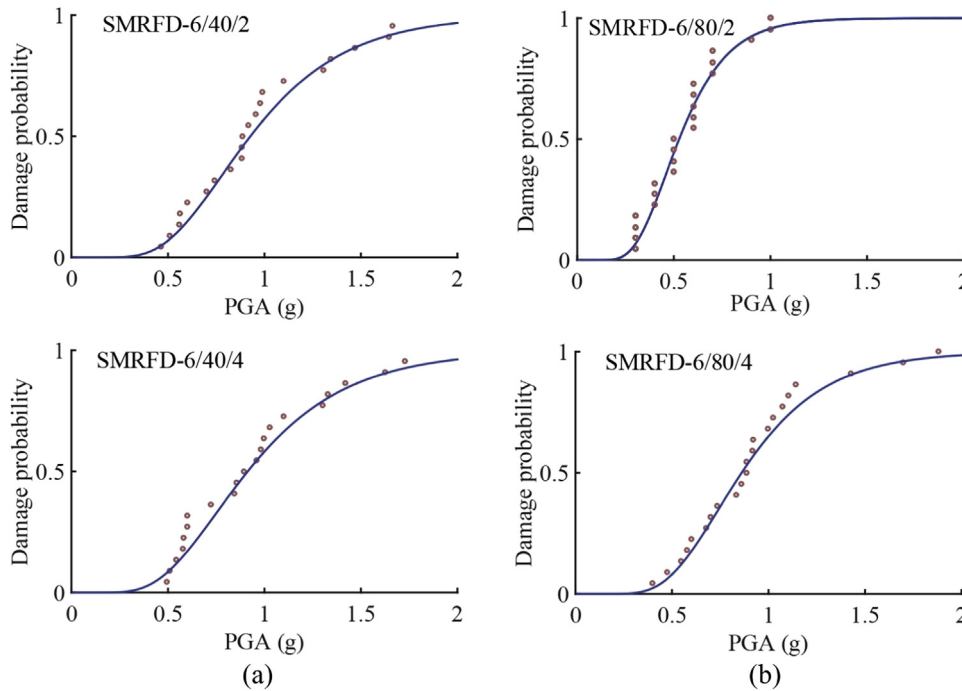


Fig. 9. Fragility curves: (a) SMRFD-6/40/2,4 and (b) SMRFD-6/80/2,4 models.

continuous curves assuming lognormal distributions are shown in Fig. 9 for the 6-story frame model with the normalized slip forces of 40% and 80% and the stiffness ratios of 2 and 4. The dotted results correspond to the empirical cumulative distribution which are fitted by the lognormal distribution (continuous curve). It can be observed that the data fit the lognormal distribution well.

Fig. 10 compares the fragility curves of the 6-story model with the

normalized slip forces of 40% and 80% and the stiffness ratios of 1–5. As shown, the damage probability of the frame having the lower  $\bar{F}_s$  (i.e. 40%) is practically not influenced by the SR variation; however, in the higher  $\bar{F}_s$  (i.e. 80%), the increase of SR reduces considerably the damage probability. In addition, the largest damage probability corresponds to the model with the higher  $\bar{F}_s$  and the lowest SR. The overall reason for these observations stems from the fact that when the

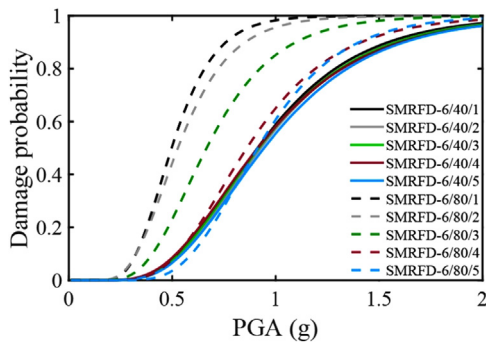


Fig. 10. Comparison of fragility curves for SMRFD-6/40/1,2,3,4,5 and SMRFD-6/80/1,2,3,4,5 models.

threshold load of the friction damper for the onset of slippage is relatively high (higher value of  $\bar{F}_s$ ) but the supporting brace is not strong enough to remain elastic during an earthquake (lower value of  $SR$ ), the undesirable buckling failure will govern before the activation of the hysteretic behavior of the damper device. As a result of such behavior,

the damage probability of the structure can increase significantly. Referring again to Figs. 7 and 8, it can be seen that the above-mentioned scenario has happened to SMRFD-6/80/2 model, where the IDA curves in most ground motion records flatten out in their maximum  $IM$  levels, signaling the onset of global dynamic instability due to the buckling of the braces.

In order to identify the optimal damper design, the  $IM$  levels corresponding to 50% damage probability (i.e., the median values of  $IM$  in the fragility functions) are computed in the entire design space of the variables  $\bar{F}_s$  and  $SR$  for the 3, 6 and 9-story structural models. The results are shown in Fig. 11, where again both  $PGA$  and  $S_a(T_1, 5\%)$  have been proposed as the  $IM$ . However, from this figure, it is easily seen that the choice of  $IM$ , whether  $PGA$  or  $S_a(T_1, 5\%)$ , does not significantly influence the variation of the objective function with respect to the design variables. A higher median  $IM$  level means a smaller probability of damage, implying a better design of the damper system. Fig. 11 shows that in order to keep the median  $IM$  level high, the upper left-hand corner of the design space should be avoided in all cases studied. This undesirable domain, which becomes larger as the number of stories decreases, corresponds to small values of  $SR$  together with large values of  $\bar{F}_s$ . Such a situation leads to insufficient energy dissipation due

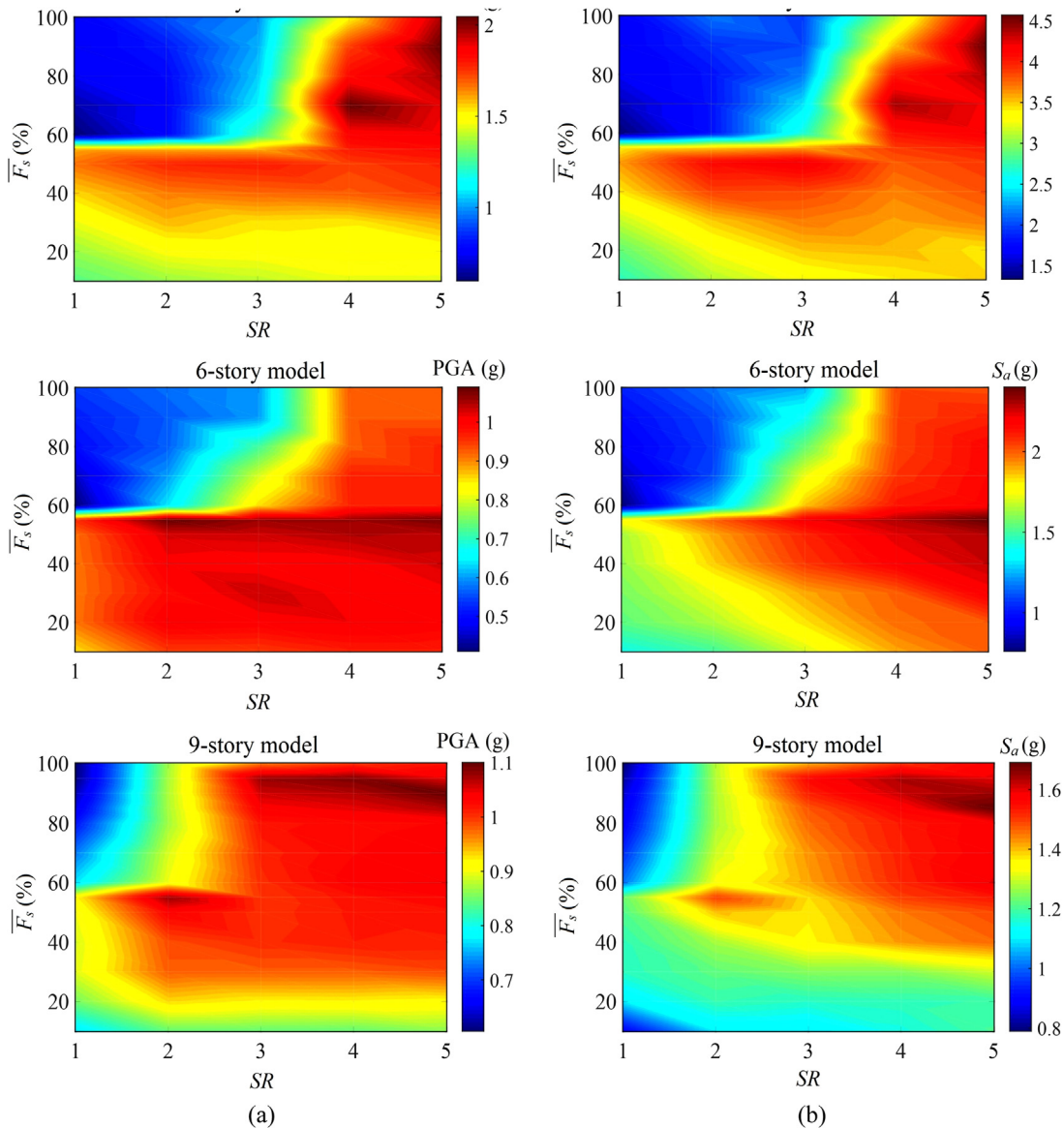


Fig. 11. The  $IM$  level with 50% probability of damage in the entire design space; (a)  $IM = PGA$  and (b)  $IM = S_a(T_1, 5\%)$ .

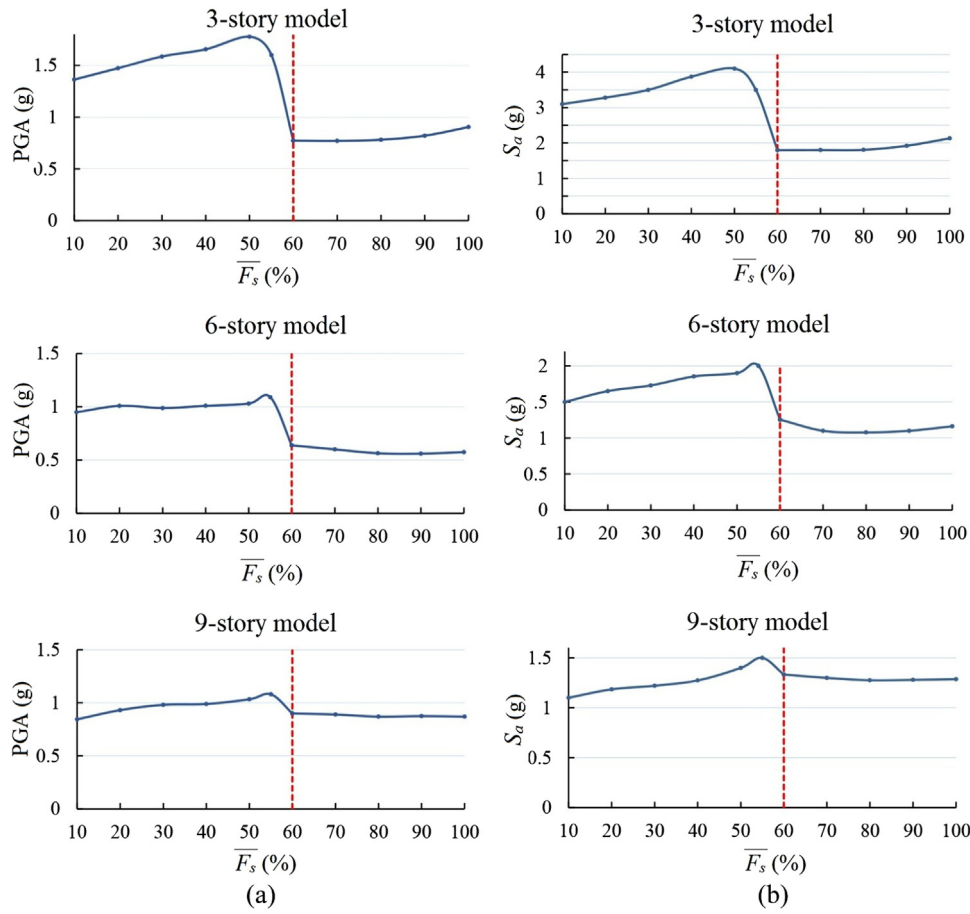


Fig. 12. The IM level with 50% probability of damage for SR = 2; (a) IM = PGA and (b) IM =  $S_a(T_1, 5\%)$ .

**Table 2**  
Estimated optimum normalized slip forces based on the spectra method proposed by Filiatrault and Cherry.

Model	$T_u$ (s)	$T_b$ (s)	$\bar{F}_s$ (%)
3-story	0.46	0.29	41
6-story	0.94	0.58	46
9-story	1.27	0.79	48

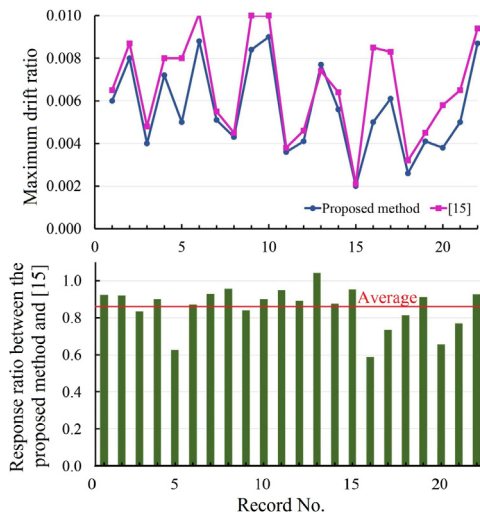


Fig. 13. Maximum inter-story drifts achieved by the two methods for the 3-story model.

to brace buckling prior to full activation of friction dampers, as previously demonstrated and discussed in detail for the 6-story building model.

The peak points on the contours in Fig. 11 correspond to the optimal choices of design parameters in building models with the different number of stories. However, one can see that the choices in the range of  $40\% \leq \bar{F}_s \leq 55\%$  with  $SR \geq 2$  lead to relatively good results for all models. A larger SR helps to some extent, but it corresponds to an increase in the size of bracing elements and thus an increase in the steel work cost. To avoid this additional cost, one can choose the smallest possible value of SR, e.g.,  $SR = 2$ .

The results of Fig. 11 are presented again in Fig. 12 with more details for the particular case of  $SR = 2$ . It is seen that in this case, the optimal values of  $\bar{F}_s$  are 50%, 55% and 55% for the 3, 6 and 9-story models, respectively. The sudden drop observed in the curves after the optimum ranges is likely related to the buckling of braces prior to the full activation of damper devices which results in a poor seismic performance of the structure and consequently an increase in the damage probability. To be sure, we calculate the minimum theoretical buckling strength of the bracing system in each frame model. The horizontal component of this force normalized to the story weight, which is comparable to  $\bar{F}_s$ , has been indicated with a vertical dotted line for each frame model in Fig. 12. It is seen that, as expected, the calculated values correspond to the dropped regions.

### 7. Comparison with an existing design method

In this section, the design parameters of the friction dampers in the assumed structural models are obtained using spectra method developed by Filiatrault and Cherry [15] for the purpose of comparison. It is

a simplified and systematic design methodology that was intended for practicing engineers. According to this method, the optimum total slip force of all friction dampers in a given multi-story structure, which is distributed uniformly over the height of the structure, is a function of the key parameters that define a particular structure under the action of strong ground motions. Each particular set of values for  $n_s$  and  $T_b/T_u$  determines a bilinear design slip force spectrum, while  $n_s$ ,  $T_b$  and  $T_u$  represent the number of stories and the natural period of braced and unbraced structures, respectively. Filiatrault and Cherry obtained the optimal slip forces of friction dampers by a direct parametric variation analysis and then used a curve fitting technique to construct these general design slip force spectra.

For the parametric study, they created and used a specialized computer program which was named as Friction Damped Braced Frame Analysis Program (FDBFAP). FDBFAP assumes the inelastic deformations of a structure to be concentrated only at the friction elements slipped and at the braces buckled in compression. For each specified slip load distribution, the program calculates energy response of the structure and determines a defined performance index based on the energy concept. The optimum slip load distribution of the structure is selected as one that produces a minimum performance index. The results of the parametric study on several multi-story friction-damped braced frames with different number of stories were used by Filiatrault and Cherry to construct the general design slip load spectra.

Using the design slip force spectra for the three structural models with ground motions considered in the present study, the optimal normalized slip forces for the stiffness ratio  $SR = 2$  are calculated and listed in Table 2. As it can be seen, the optimal values of the slip force calculated based on the spectra method fall within the recommended ranges of this variable by our proposed method. However, they are not exactly the same as our obtained optimal values in the previous section (i.e. 50%, 55%, and 55% for 3, 6, and 9-story models) and consequently, the damage potentials corresponding to these values will be larger than the minimum levels resulted from the proposed method. To be sure, one can compare the  $IM$  levels of 50% damage probability for the optimum choices of  $\bar{F}_s$  in the two methods. For the 3, 6, and 9-story models these PGA levels are 1.67 g, 1.02 g, and 1.02 g, respectively, when assuming the choices of the spectra method, while they are the maximum levels of 1.78 g, 1.09 g, and 1.08 g, respectively, according to the proposed method. This means that when the damage-based method replaces the spectra method, the median  $IM$  level of the fragility function increases by about 6%.

Fig. 13 compares the maximum inter-story drift ratios achieved by the two methods in the 3-story model subjected to each selected ground motion. To make the results of different records comparable, each ground motion has been scaled to 50% of its final  $IM$  level of the IDA procedure for the 3-story model. It is seen from Fig. 13 that the damage-based design solution is also effective in reducing the maximum drift ratios. This figure also shows the drift response ratio between the values obtained from the proposed method and the spectra method. As it can be seen, in most cases the values are less than one indicating that the design solution obtained by minimizing the damage probability provides lower maximum inter-story drifts. The average reduction is 15%.

## 8. Conclusions

In this paper, a damage-based approach was proposed to evaluate the optimal range of design parameters of friction dampers in multi-story chevron braced steel frames. To demonstrate the efficiency of the proposed method, three structural models equipped with friction damper systems were evaluated using IDA procedure. Seismic fragility analysis of the structural models was performed by changing their two design variables: the normalized slip force of damper device  $\bar{F}_s$  and the stiffness ratio of the damper system  $SR$ . The obtained results can be interpreted to improve the knowledge on this kind of structures as well as to identify an optimal range of variables. The main findings of these

numerical analyses can be summarized as follows:

- The fragility data obtained using the IDA procedure fit the log-normal distribution well.
- The damage potential of a frame having lower  $\bar{F}_s$  is not affected by the  $SR$  variation; however, in the case of using higher  $\bar{F}_s$ , the results are highly dependent to the  $SR$  variation. Generally, the largest damage probability corresponds to a frame with higher  $\bar{F}_s$  and lower  $SR$ .
- The choice of  $IM$ , whether PGA or  $S_a(T_1, 5\%)$  does not significantly influence the variation of the objective function with respect to the design variables.
- Considering the proposed damage-based methodology, the optimal ranges of friction damper parameters installed in steel moment-resisting frames lie in the range of  $40\% \leq \bar{F}_s \leq 55\%$  with  $SR \geq 2$ .
- Increasing the  $SR$  will reduce the damage potential, but it corresponds to an increase in the size of bracing elements and thus an increase in the steel work cost. To avoid this additional cost, it is suggested to choose the smallest possible value, i.e.,  $SR = 2$ .
- Comparison of the numerical results obtained using the proposed method with the spectra method developed by Filiatrault and Cherry shows that the damage potentials corresponding to the values resulted from the spectra method are larger than the minimum levels resulted from the proposed method. In addition, our design solution obtained by minimizing the damage probability provides lower maximum inter-story drifts.

## References

- [1] Soong TT, Dargush GF. *Passive energy dissipation systems in structural engineering*. Chichester: John Wiley and Sons Ltd.; 1997.
- [2] Pall AS, Marsh C. Response of friction damped braced frames. *J Struct Eng ASCE* 1982;108(6):1313–23.
- [3] Pall AS, Verganelakis V, Marsh C. Friction dampers for seismic control of Concordia University library building. In: Proceedings of the fifth Canadian conference on earthquake engineering. Ottawa, Canada; 1987, p. 191–200.
- [4] Monir HS, Zeynali K. A modified friction damper for diagonal bracing of structures. *J Constr Steel Res* 2013;87:17–30.
- [5] Montuori R, Nastri E, Piluso V, Streppone S. The use of TPMC for designing MRFs equipped with FREEDAM connections: performance evaluation. *Key Eng Mater* 2018;763:983–91.
- [6] Latour M, Piluso V, Rizzano G. Free from damage beam-to-column joints: testing and design of DST connections with friction pads. *Eng Struct* 2015;85:219–33.
- [7] Aiken ID, Kelly JM. Earthquake simulator testing and analytical studies of two energy-absorbing systems for multistory structures [Report no. UCB/EERC-90/03]. Berkeley: University of California; 1990.
- [8] Gregorian CE, Yang TS, Popov EP. Slotted bolted connection energy dissipaters. *Earthq Spectra* 1993;9(3):491–504.
- [9] Nims DK, Inaudi JA, Richter PJ, Kelly JM. Application of the energy dissipating restraint to buildings. In: Proceedings of the ATC 17-1 on seismic isolation, energy dissipation, and active control; 1993, p. 627–38.
- [10] Zhou X, Peng L. A new type of damper with friction-variable characteristics. *Earthq Eng Vib* 2009;8(4):507–20.
- [11] Mualla IH, Belev B. Performance of steel frames with a new friction damper device under earthquake excitation. *Eng Struct* 2002;24(3):365–71.
- [12] Golafshani AA, Tabeshpour MR, Komachi Y. FEMA approaches in seismic assessment of jacket platforms (case study: Ressalat jacket of Persian Gulf). *J Constr Steel Res* 2009;65(10–11):1979–86.
- [13] Tapia N, Almazán J, Baquero J. Development of a novel combined system of deformation amplification and added stiffness and damping: analytical result and full scale pseudo-dynamic tests. *Eng Struct* 2016;119:61–80.
- [14] Filiatrault A, Cherry S. Efficient numerical modelling for the design of friction damped braced steel plane frames. *Can J Civ Eng* 1989;16(3):211–8.
- [15] Filiatrault A, Cherry S. Seismic design spectra for friction-damped structures. *J Struct Eng ASCE* 1990;116(5):1334–55.
- [16] Fu Y, Cherry S. Design of friction damped structures using lateral force procedure. *Earthq Eng Struct Dyn* 2000;29(7):989–1010.
- [17] Lopez Garcia D, Soong TT. Efficiency of a simple approach to damper allocation in MDOF structures. *J Struct Control* 2002;9(1):19–30.
- [18] Moreschi LM, Singh MP. Design of yielding metallic and friction dampers for optimal seismic performance. *Earthq Eng Struct Dyn* 2003;32(8):1291–311.
- [19] Lee SH, Park JH, Lee SK, Min KW. Allocation and slip load of friction dampers for a seismically excited building structure based on storey shear force distribution. *Eng Struct* 2008;30(4):930–40.
- [20] Pall A, Pall RT. Performance-based design using pall friction dampers -an economical design solution. In: Proceedings of the 13th world conference on earthquake engineering. Vancouver, Canada; 2004.

- [21] Baker JW. Efficient analytical fragility function fitting using dynamic structural analysis. *Earthq Spectra* 2015;31(1):579–99.
- [22] Vamvatsikos D, Cornell CA. Incremental dynamic analysis. *Earthq Eng Struct Dyn* 2002;31(3):491–514.
- [23] Zareian F, Krawinkler H. Assessment of probability of collapse and design for collapse safety. *Earthq Eng Struct Dyn* 2007;36(13):1901–14.
- [24] AISC 360. Specification for structural steel buildings [ANSI/AISC 360-10]. Chicago, IL: American Institute of Steel Construction; 2010.
- [25] ASCE 7. Minimum design loads for buildings and other structures [ASCE/SEI 7-10]. Reston, VA: American Society of Civil Engineers; 2010.
- [26] Modeling of Pall friction dampers. Pall Dynamics Limited; 2018. <<http://www.palldynamics.com>>.
- [27] FEMA-P695. Quantification of building seismic performance factors. Washington, DC: Federal Emergency Management Agency; 2009.